Solar Phys (2019) 294:26
https://doi.org/10.1007/s11207-019-1409-7

Characteristics of the Solar Coronal Line Profiles from Fabry–Perot Interferometric Observations

Maya Prabhakar[1] · **K.P. Raju**[1] · **T. Chandrasekhar**[2]

Received: 12 September 2018 / Accepted: 2 February 2019 / Published online: 1 March 2019

Abstract This article reports the analysis of a set of Fabry–Perot interferograms that were studied to probe the physical parameters of the inner solar corona. The observations were carried out in the coronal green line, Fe XIV 5302.86 Å, during the total solar eclipse of 21 June 2001 that occurred in Lusaka, Zambia. The study was performed in the radial range of 1.1 – 1.5 $R_{\odot}$ and examines the Doppler velocity, half-width, centroid, and asymmetry and their correlations with each other at various points in the corona. We found that 59% of the line profiles are blueshifted, 34% are single components, and only 7% are redshifted. The variations in half-width and Doppler velocity with respect to coronal height have a large scatter and show no significant changes. We found that the variation in half-width with Doppler velocity or centroid follows a parabolic trend with a weak correlation, whereas the relation between half-width and asymmetry is inconclusive. These results may provide more insight into the coronal dynamics and help in understanding the physical problems in the corona.

Keywords Corona, E · Eclipse observations · Spectral line, broadening · Spectrum, visible

1. Introduction

The transition region and the solar corona are widely explored for their several intriguing features. The dynamics of the flows and mass motions, the multiple component line profiles, line shifts and their dominance, nonthermal velocities and intensity variations at different

✉ M. Prabhakar
maya.prabhakar@iiap.res.in

K.P. Raju
kpr@iiap.res.in

T. Chandrasekhar
chandra@prl.res.in

1 Indian Institute of Astrophysics, Bangalore, India

2 Physical Research Laboratory, Ahmedabad, India

regions are a few topics that are widely discussed. Most studies of these topics aimed at determining whether they can provide any insight into coronal heating and the solar wind acceleration. The solar corona has been an interesting region: it has a very low density of the order of 10^{8-9} cm^{-3} and a temperature of the order of 2 MK. Many theories such as nanoflare heating, type-II spicules, magnetic reconnection, and Alfvén waves have been proposed to explain this high temperature (Sakurai, 2017). The study continues in search of nonthermal energy sources that might cause coronal heating and the solar wind acceleration. Studying the solar coronal line profiles is one such method, where we can gain information about the physical parameters of the solar corona.

Asymmetries have generally been reported in spectral lines from the transition region and the solar corona. Mass motions in the corona have been reported by Delone and Makarova (1969, 1975), Delone, Makarova, and Yakunina (1988) and Chandrasekhar *et al.* (1991). Multiple components with excess blueshifts have been reported by Raju *et al.* (1993). Brynildsen, Kjeldseth-Moe, and Maltby (1995) described the increasing fraction of redshifts in the transition region. Brekke, Hassler, and Wilhelm (1997) and Teriaca *et al.* (1999) reported that the transition region comprises redshifts. Chae, Yun, and Poland (1998) and Peter and Judge (1999) also found excess blueshifts through Solar Ultraviolet Measurements of Emitted Radiation (SUMER) observations. Raju (1999) showed the existence of multiple components in the line profiles. Dadashi, Teriaca, and Solanki (2011) also found excess blueshifted profiles in the corona. Patsourakos and Klimchuk (2006) explained these emissions in terms of nanoflare heating, and De Pontieu *et al.* (2009) related them to type-II spicules. Brooks and Warren (2012) explained these asymmetries as signatures of chromospheric jets that provide mass and energy to the corona.

Furthermore, the results regarding the variation in nonthermal velocity and line width with height were different. The line width of the red line was reported to increase with height above the limb by Singh *et al.* (2006). Prasad, Singh, and Banerjee (2013) presented a negative gradient of the green line width with height. Raouafi and Solanki (2004) reported an anisotropy of the velocity distribution in this region. The nature of the variation in line profile parameters is still unclear, and in this paper, we aim to study it in more detail.

In this context, we have focused on the physical parameters of the solar corona, such as Doppler velocity, half-width, centroid, and asymmetry and their correlations at various points away from the limb by analyzing a set of Fabry–Perot interferograms. We have primarily focused on the variation in Doppler velocity and centroid of the line widths of the line profiles. This work is a continuation of our earlier work (Prabhakar, Raju, and Chandrasekhar, 2013), which mainly focused on the shifts and asymmetries of the line profiles. Section 2 gives details of the instrument used and of the analysis and data reduction methods involved in our study. In Section 3 we describe the results we found in our study and discuss them in comparison to the earlier results. Section 4 gives the conclusion of our study.

2. Analysis and Data Reduction

Our study involves the analysis of 14 Fabry–Perot interferograms. These were taken during the total solar eclipse that occurred in Lusaka, Zambia, on 21 June 2001. It had a magnitude of 1.0495 and lasted for 3 min 37 sec when the Sun was at 31° elevation above the northwest horizon. From the data, we have obtained the intensity, Doppler velocity, half-width, centroid, and asymmetry at different points in the corona. The centroid is defined as the wavelength point that divides the area of the line profile into two (Raju, Chandrasekhar, and Ashok, 2011). To calculate the asymmetry, strips of equal width (0.5 Å) at equal distances

Table 1 Instrumental features of the Fabry–Perot interferometer.

Features	Values
Free spectral range	4.75 Å
Instrumental width	0.2 Å
Spectral resolution	26,000
CCD configuration	1024 × 1024
Pixel size	24 μm
Pixel resolution	3.4 arcsec

(0.1 Å) from the peak wavelength were considered in the red (R) and blue (B) regions. The asymmetry was then calculated using the relation $(R - B)/(R + B)$. The observation was made in the coronal green line Fe XIV 5302.86 Å, which was chosen because its formation temperature (2 MK) is close to the average inner coronal temperature. This means that the results yield more accurate information about the corona.

The Fabry–Perot interferometer we used is the one used in Chandrasekhar *et al.* (1984). However, during the 21 June 2001 eclipse, a CCD was used as the detector. The interferometer has a free spectral range of 4.75 Å, an instrumental width of 0.2 Å, a spectral resolution of 26,000 for the coronal green line, and a pixel resolution of 3.4 arcsec. The instrumental details are given in Table 1. The line profiles were extracted in the angular range of 240°. The original plan of the experiment was to obtain a time-sequence of Fabry–Perot interferograms of the solar corona during the total solar eclipse. The aim was to study the temporal changes in the physical properties of the solar corona. However, as a result of a minor tracking error that happened during the observation, it was later noted that the interferograms were not cospatial. Hence, we could not study the temporal variations. However, this enabled us to study the corona at more spatial locations than was originally planned.

In a Fabry–Perot interferogram, the region between two adjacent fringe minima constitutes a line profile. The spatial resolution in an imaging Fabry–Perot interferometer is therefore generally low. It is about 0.2 $R_\odot$ in our observation. The tracking error in the observation will shift an interferogram with respect to the previous one, leading to the formation of a new fringe pattern in the gap. This will give line profiles from new locations, but with some boxcar averaging of the nearby spatial points. The angular coverage therefore remains the same (240°) as in a single interferogram, but we obtain more line profiles from the intermediate regions. Part of the data obtained during this particular eclipse was used by Raju, Chandrasekhar, and Ashok (2011) and Prabhakar, Raju, and Chandrasekhar (2013).

The analysis was made by first locating the fringe center position in the interferograms. Then the radial scans from the fringe center were made to obtain the line profiles. The wavelength was calibrated as in Raju *et al.* (1993). In order to reduce the noise, a 2 × 2 pixel averaging was made at the outset. It was also noted that the line profiles close to the limb were slightly contaminated by the scattered light in some interferograms. Therefore we considered only line profiles beyond 1.1 $R_\odot$. Single Gaussian curves were fit to all the line profiles and the parameters were obtained. We selected only line profiles whose signal-to-noise ratio was ≥ 15 in order to obtain good Gaussian fits. A set of line profiles fitted with Gaussian curves is shown in Figure 1. The estimated errors in the fitting are about 5% in intensity, 2 km s^{-1} in velocity, and 0.03 Å in width. Interactive Data Language (IDL) was used for computation purposes. All the spatial locations of the line profiles obtained are plotted on an *Extreme ultraviolet Imaging Telescope* (EIT) image of the Sun obtained at the same time as that of the eclipse, which is shown in Figure 2.

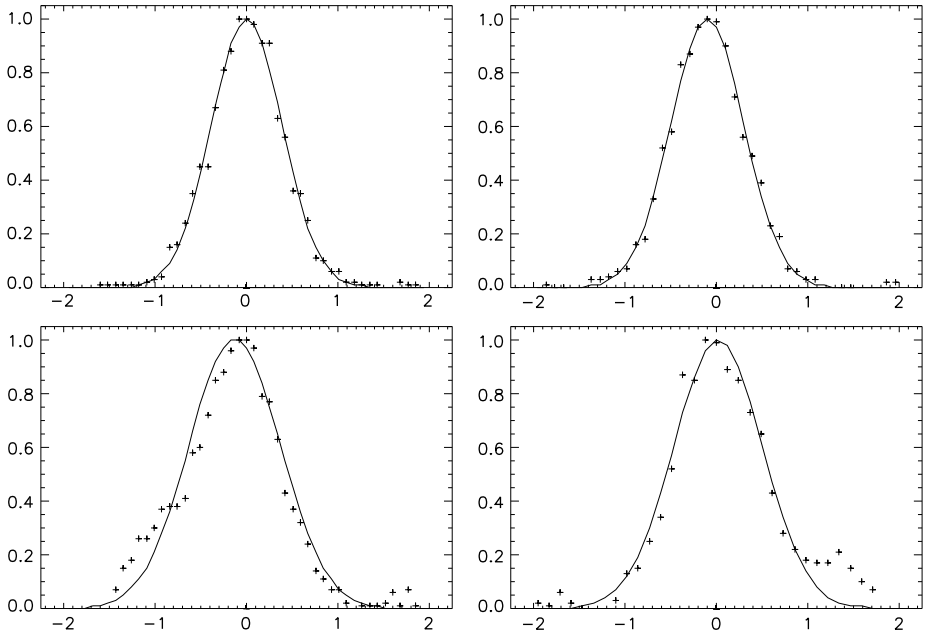

Figure 1 Example of line profiles fitted with Gaussian curves. The *upper two line* profiles represent single component profiles, and the *lower two* represent blueshifted (*left*) and redshifted (*right*) line profiles.

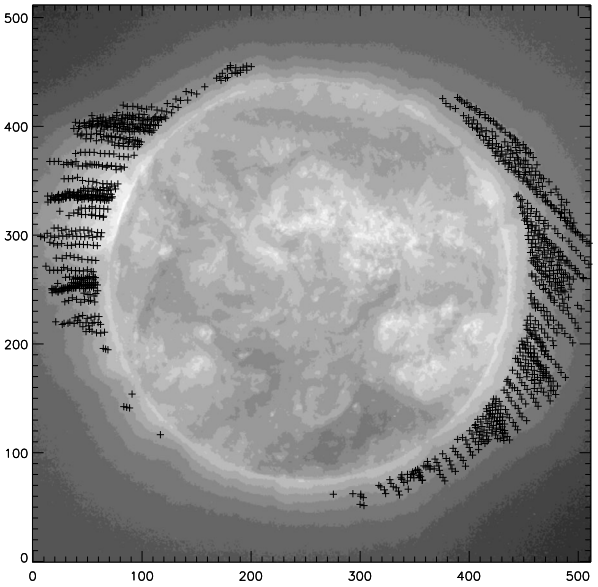

Figure 2 EIT image of the Sun on 21 June 2001 at time 13:48:13, showing the spatial locations of all the line profiles we analyzed.

3. Results and Discussion

We obtained 1295 line profiles in all by removing the noisy profiles. We found that 59% of them are blueshifted, 7% are redshifted, and 34% are single components. Single components

Table 2 Number of line profiles observed in different ranges of asymmetry.

Type	Asymmetry range (Å)	Number of profiles	Total
Single	−0.08 to 0.08	439	34%
Blueshifts	−0.08 to −0.2	428	
	−0.2 to −0.3	237	
	−0.3 to −0.6	96	59%
Redshifts	0.08 to 0.2	76	
	0.2 to 0.3	19	7%

are those that fall in the asymmetry range of $-0.08-0.08$ Å, corresponding to the Doppler velocity range of $-2-2$ km s^{-1}. It is interesting to see that the percentages of the single components, blueshifts, and redshifts are different from what was observed in Raju, Chandrasekhar, and Ashok (2011) and Prabhakar, Raju, and Chandrasekhar (2013). Note that the above works considered almost 300 line profiles. In this work, the improved statistics give a better reliability (a factor of about 2) to our results than in the works mentioned above.

This work is primarily focused on the variations in Doppler velocity, half-width, centroid, and asymmetry and their interrelationships. The gross properties of a large number of line profiles fitted with a single Gaussian were obtained. By examining the interrelationships between the quantities, we expect to receive information on the nature of the multiple components without requiring complex multiple Gaussian fitting. Raju, Chandrasekhar, and Ashok (2011) obtained line profiles from a single interferogram and the nature of the secondary component, obtained by subtracting the red from the blue wing, was studied in detail. Prabhakar, Raju, and Chandrasekhar (2013) primarily studied the asymmetry of the multiple components.

The number of line profiles observed in different asymmetry ranges is given in Table 2. The line profiles with the greatest asymmetry are found in the blue wing (96 line profiles). Thus, our results agree well with the works by Raju *et al.* (1993), Raju (1999), Dadashi, Teriaca, and Solanki (2011), Chae, Yun, and Poland (1998), and Peter and Judge (1999) regarding the presence of the multiple components and dominance of the blueshifts, but the percentage is found to be on the higher side. The redshifts are seen to be very less, with a contribution of just 7%.

The normalized histograms of Doppler velocity, centroid, and asymmetry of the line profiles are shown in Figure 3. All of them show the domination of the blueshifts, which does not agree with McIntosh *et al.* (2012), who reported a weak emission component in the blue wing that contributes a very low percentage of the emission line profiles. The multiple components with blueshifts are found to have a maximum Doppler velocity of -18 km s^{-1}, and those with redshifts are found to have a maximum Doppler velocity of 11 km s^{-1}. It is to be noted that these values are taken from the composite line profiles, and when the Gaussian decomposition is performed, the velocities of the secondary components are much higher (Raju, Chandrasekhar, and Ashok, 2011).

The normalized histogram of the half-width is shown in Figure 4. The half-width falls in the range $0.7-1.3$ Å and the peak at 0.96 Å. This would correspond to a temperature of 3.5 MK. Considering the nonthermal broadening that could add to the line width and the line formation temperature of 2 MK, we find that the nonthermal velocity is close to 22 km/s (Raju, Chandrasekhar, and Ashok, 2011) from the following relation:

$$\frac{2kT_0}{M} = \frac{2kT_D}{M} + v_t^2,$$

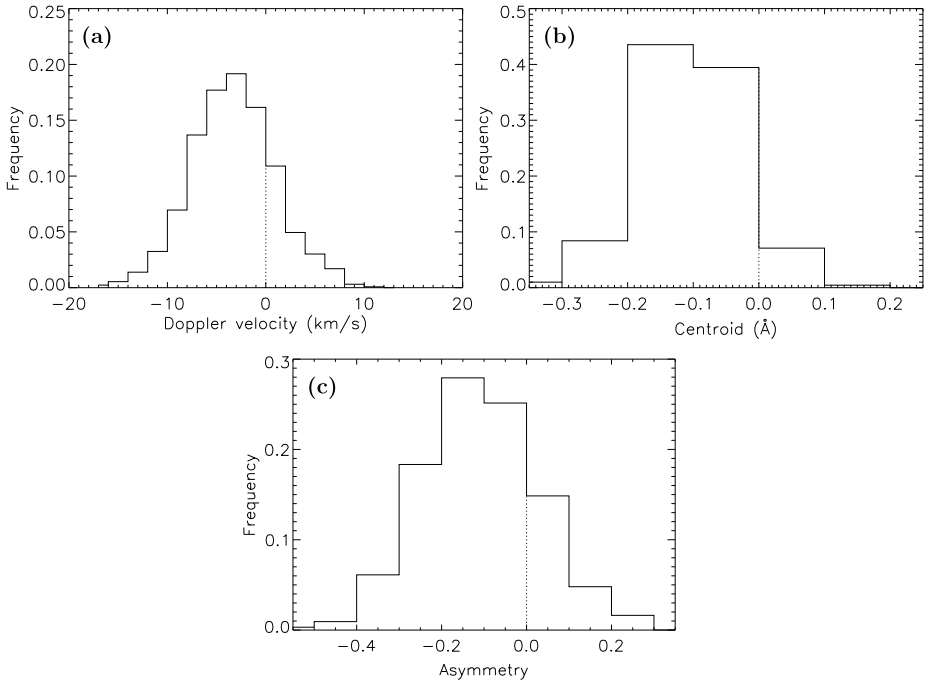

Figure 3 Normalized histograms of (**a**) the Doppler velocity, (**b**) the centroid, and (**c**) the asymmetry.

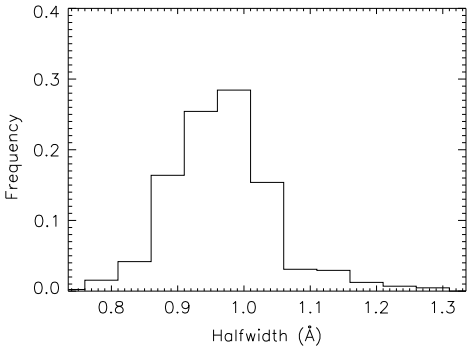

Figure 4 Normalized histogram of the half-width of the line profiles.

where k is the Boltzmann constant, T_0 is the observed line-width temperature, M is the mass of the emitting ion, $T_{\rm D}$ is the Doppler temperature of the line width, and $v_{\rm t}$ is the nonthermal velocity characterizing microturbulence.

Furthermore, we studied the variation in half-width and Doppler velocity of the line profiles with respect to their heights from the solar center. In Figure 5a, we plot the half-width against the coronal height. We have tried linear, quadratic, and cubic polynomial fits, and a detailed statistical analysis was performed. The details are given in Table 3. The different columns in the table give the values of the correlation coefficient (R), the coefficient of the determination (R^2), and the standard error in the fittings. The table shows that the best fit is obtained from the cubic polynomial fit, where the value of $R = 0.21$ and $R^2 = 4.4\%$.

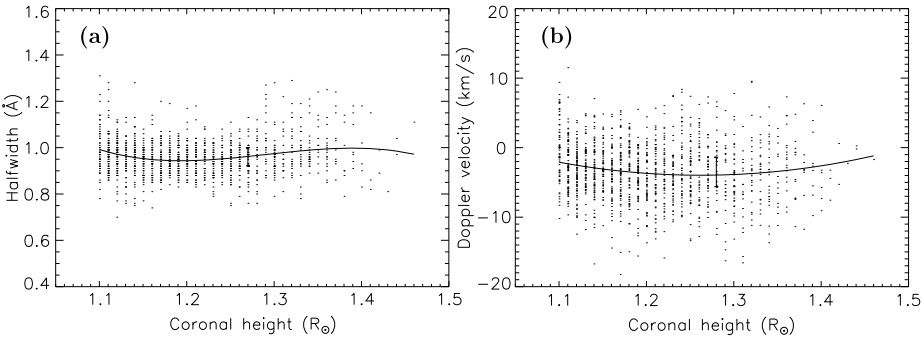

Figure 5 (**a**) Variation in half-width and (**b**) Doppler velocity with height above the limb. The *solid line* shows the best-fit polynomial. The *error bar* indicates the standard error in the fittings.

Table 3 Values of R, R^2, and standard errors for the plots in Figures 5 and 6 for linear, quadratic, and cubic fittings.

Figure	Linear			Quadratic			Cubic		
	R	R^2	standard error	R	R^2	standard error	R	R^2	standard error
Figure 5a	0.05	0.0025	0.07	0.18	0.031	0.078	0.21	0.044	0.078
Figure 5b	−0.08	0.0068	4.26	0.14	0.018	4.23	0.14	0.021	4.23
Figure 6a	0.03	0.0008	0.079	0.23	0.051	0.077	0.22	0.048	0.077
Figure 6b	0.02	0.0004	0.079	0.21	0.045	0.078	0.21	0.045	0.078
Figure 6c	0.12	0.015	0.079	0.12	0.014	0.079	0.12	0.015	0.079

The best-fit polynomial and the standard error are plotted in the figure. The total variation is comparable to the standard error in the fitting, and the trend is therefore insignificant.

This result is different from what is observed in Mierla *et al.* (2008), who stated that the width remains almost constant or increases up to a height of 1.3 $R_\odot$. It is also different from what was described in Prasad, Singh, and Banerjee (2013) and Beck *et al.* (2016), who reported a decrease in line widths with height of the line profiles.

Figure 5b shows the variation in Doppler velocity of the line profiles with coronal height. Table 3 shows that the coefficients R and R^2 do not show much improvement from quadratic to cubic fits. A quadratic fit was therefore considered for this plot. Here the total variation is less than the standard error and hence insignificant.

We further studied the variation in half-width of the line profiles with Doppler velocity and centroid, which are shown in Figure 6a and b. From Table 3, it is evident that the quadratic fit is better than the linear fit, where the coefficients show a marked improvement. There is no marked improvement in the cubic fit. The total variation is almost twice the standard error, and these fits were therefore retained. The correlation coefficients are 0.23 and 0.21 for velocity and centroid, respectively, which means a mild correlation. The R^2 values, which give the percentage of this variation, are about 5%. This implies that the relationship between half-width and Doppler velocity or centroid is weak. A variation like this was observed in Bryans, Young, and Doschek (2010) for Active Region AR 10978. Raju, Chandrasekhar, and Ashok (2011) examined the relationship between half-width and Doppler velocity from two cases with a limited number of samples and a positive angle coverage

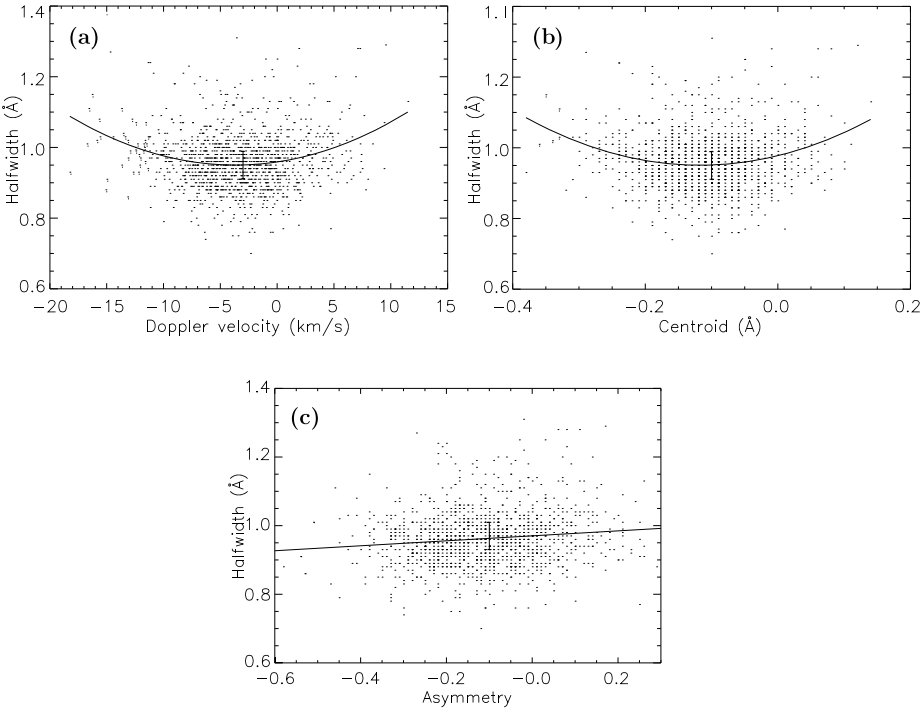

Figure 6 (**a**) Variation in Doppler velocity, (**b**) centroid, and (**c**) asymmetry of the line profiles with half-width. The *solid line* shows the best-fit polynomial. The *error bar* indicates the standard error in the fittings.

of 20°. They reported a weak correlation in one case and a lack of correlation in the other. It may therefore be concluded that the weak correlation found between the half-width and Doppler velocity or centroid could be real. Peter (2010) reported that the positive correlation between these quantities suggests a flow associated with a heating process.

The variation in half-width with respect to the asymmetry of the line profiles is given in Figure 6c. Here the quadratic or cubic fit do not improve the linear fit. The coefficients R, R^2, and standard error remain almost constant in all the three cases. The linear trend is comparable to the standard error and is not significant. This is found to be very different when compared to the variation in Doppler velocity and centroid with half-width.

4. Conclusion

We studied various characteristics of the inner solar corona by analyzing the line profiles obtained from the analysis of Fabry–Perot interferograms. We found that a majority of these line profiles comprise multiple components, with a higher contribution from blueshifts (59%). This is followed by single-component profiles, which contribute 34%. Redshifts contribute very little, just 7%. This result, although found to be in agreement with related works reported earlier, shows a very high percentage of blueshifts. Line profiles showing the greatest asymmetry were found to be blueshifted, and they constitute close to 7.5% of the observed line profiles. The multiple component profiles with blueshifts were found to have a

maximum Doppler velocity of -18 km s^{-1}, and the redshifted multiple components were found to have a maximum Doppler velocity of 11 km s^{-1}. These values specify the Doppler velocity of the composite profile, and the actual values of the Doppler velocity of the components could be much higher. The excess blueshifts could be related to type-II spicules or to the nascent solar wind flow. Furthermore, the variation in half-width and Doppler velocity with respect to the coronal height are found to be insignificant. The variation in half-width with respect to the Doppler velocity or centroid shows a parabolic trend with a weak correlation. The positive correlation is important because it suggests a flow that is associated with a heating process. The trend between half-width and asymmetry is inconclusive, which is not understood. These results need to be examined further to understand the problems in coronal physics.

Acknowledgements The authors would like to thank the reviewer for their valuable comments and suggestions. Maya Prabhakar would like to thank the Women Scientist Scheme-A (WOS-A) of the Department of Science & Technology for providing financial support to carry out this project. This work is also funded by the Department of Science & Technology and by the Department of Space, Government of India.

Disclosure of Potential Conflicts of Interest The authors declare that they have no conflicts of interest.

Publisher's Note Springer Nature remains neutral with regard to jurisdictional claims in published maps and institutional affiliations.

References

Beck, C., Rezaei, R., Puschmann, K.G., Fabbian, D.: 2016, Spectroscopy at the solar limb: II. Are spicules heated to coronal temperatures? *Solar Phys.* **291**, 2281. DOI. ADS.

Brekke, P., Hassler, D.M., Wilhelm, K.: 1997, Doppler shifts in the quiet-Sun transition region and corona observed with SUMER on SOHO. *Solar Phys.* **175**, 349. DOI. ADS.

Brooks, D.H., Warren, H.P.: 2012, The coronal source of extreme-ultraviolet line profile asymmetries in solar active region outflows. *Astrophys. J. Lett.* **760**, L5. DOI. ADS.

Bryans, P., Young, P.R., Doschek, G.A.: 2010, Multiple component outflows in an active region observed with the EUV imaging spectrometer on Hinode. *Astrophys. J.* **715**, 1012. DOI. ADS.

Brynildsen, N., Kjeldseth-Moe, O., Maltby, P.: 1995, Quiet-sun connection between intensity, Doppler shift, and line broadening in solar ultraviolet emission lines. *Astrophys. J. Lett.* **455**, L81. DOI. ADS.

Chae, J., Yun, H.S., Poland, A.I.: 1998, Temperature dependence of ultraviolet line average Doppler shifts in the quiet Sun. *Astron. Astrophys. Suppl. Ser.* **114**, 151. DOI. ADS.

Chandrasekhar, T., Ashok, N.M., Desai, J.N., Pasachoff, J.M., Sivaraman, K.R.: 1984, Fabry–Perot interferometric observations of the coronal red and green lines during the 1983 Indonesian eclipse. *Appl. Opt.* **23**, 508. DOI. ADS.

Chandrasekhar, T., Desai, J.N., Ashok, N.M., Pasachoff, J.M.: 1991, Fabry–Perot line profiles in the 5303 A and 6374 A coronal lines obtained during the 1983 Indonesian eclipse. *Solar Phys.* **131**, 25. DOI. ADS.

Dadashi, N., Teriaca, L., Solanki, S.K.: 2011, The quiet Sun average Doppler shift of coronal lines up to 2 MK. *Astron. Astrophys.* **534**, A90. DOI. ADS.

De Pontieu, B., McIntosh, S.W., Hansteen, V.H., Schrijver, C.J.: 2009, Observing the roots of solar coronal heating – in the chromosphere. *Astrophys. J. Lett.* **701**, L1. DOI. ADS.

Delone, A.B., Makarova, E.A.: 1969, Interferometric investigation of the red and green coronal lines during the total solar eclipse of May 30, 1965. *Solar Phys.* **9**, 116. DOI. ADS.

Delone, A.B., Makarova, E.A.: 1975, Interferometric investigation of the line of sight velocities in the 5303-A line during the eclipse 11 September, 1968. *Solar Phys.* **45**, 157. DOI. ADS.

Delone, A.B., Makarova, E.A., Yakunina, G.V.: 1988, Erratum: "Evidence for moving features in the corona from emission line profiles observed during eclipses" [*J. Astrophys. Astron.* **9**(1), 41 – 47 (1988)]. *J. Astrophys. Astron.* **9**, 125. DOI. ADS.

McIntosh, S.W., Tian, H., Sechler, M., De Pontieu, B.: 2012, On the Doppler velocity of emission line profiles formed in the "coronal contraflow" that is the chromosphere-corona mass cycle. *Astrophys. J.* **749**, 60. DOI. ADS.

Mierla, M., Schwenn, R., Teriaca, L., Stenborg, G., Podlipnik, B.: 2008, Analysis of the Fe X and Fe XIV line width in the solar corona using LASCO-C1 spectral data. *Astron. Astrophys.* **480**, 509. DOI. ADS.

Patsourakos, S., Klimchuk, J.A.: 2006, Nonthermal spectral line broadening and the nanoflare model. *Astrophys. J.* **647**, 1452. DOI. ADS.

Peter, H.: 2010, Asymmetries of solar coronal extreme ultraviolet emission lines. *Astron. Astrophys.* **521**, A51. DOI. ADS.

Peter, H., Judge, P.G.: 1999, On the Doppler shifts of solar ultraviolet emission lines. *Astrophys. J.* **522**, 1148. DOI. ADS.

Prabhakar, M., Raju, K.P., Chandrasekhar, T.: 2013, Analysis of the solar coronal green line profiles from eclipse observations. In: *International Symposium on Solar-Terrestrial Physics*, *Astronomical Society of India Conference Series* **10**. ADS.

Prasad, S.K., Singh, J., Banerjee, D.: 2013, Variation of emission line width in mid- and high-latitude corona. *Solar Phys.* **282**, 427. DOI. ADS.

Raju, K.P.: 1999, The effect of mass motions inside the coronal loops on emission line profiles. *Solar Phys.* **185**, 311. DOI. ADS.

Raju, K.P., Chandrasekhar, T., Ashok, N.M.: 2011, Analysis of coronal green line profiles: Evidence of excess blueshifts. *Astrophys. J.* **736**, 164. DOI. ADS.

Raju, K.P., Desai, J.N., Chandrasekhar, T., Ashok, N.M.: 1993, Line-of velocities observed in the inner solar corona during the total solar eclipses of 1980 and 1983. *Mon. Not. Roy. Astron. Soc.* **263**, 789. DOI. ADS.

Raouafi, N.-E., Solanki, S.K.: 2004, Effect of the electron density stratification on off-limb O VI line profiles: How large is the velocity distribution anisotropy in the solar corona? *Astron. Astrophys.* **427**, 725. DOI. ADS.

Sakurai, T.: 2017, Heating mechanisms of the solar corona. *Proc. Japan Acad. Ser. B* **93**, 87. DOI. ADS.

Singh, J., Sakurai, T., Ichimoto, K., Muneer, S.: 2006, Spectroscopic studies of solar corona VI: Trend in line-width variation of coronal emission lines with height independent of the structure of coronal loops. *J. Astrophys. Astron.* **27**, 115. DOI. ADS.

Teriaca, L., Banerjee, D., Doyle, J.G., Erdély, R.: 1999, SUMER observations of line shifts in the quiet sun and in an active region. In: Vial, J.-C., Kaldeich-Schü, B. (eds.) *8th SOHO Workshop: Plasma Dynamics and Diagnostics in the Solar Transition Region and Corona*, *ESA Special Publication* **446**, 645. ADS.